Interlaminar toughening of resin transfer moulded glass fibre epoxy laminates by polycaprolactone electrospun nanofibres

Sam van der Heijden [a] , Lode Daelemans [a], Bert De Schoenmaker [a], Ives De Baere [b], Hubert Rahier [c], Wim Van Paepegem [b], Karen De Clerck [a*]

[a] Ghent University, Department of Textiles, Technologiepark-Zwijnaarde 907, B-9052 Zwijnaarde, Belgium

[b] Ghent University, Department of Materials Science and Engineering, Technologiepark-Zwijnaarde 903, B-9052 Zwijnaarde, Belgium

[c] Vrije Universiteit Brussel, Department Materials and Chemistry, Pleinlaan 2, B-1050 Brussels, Belgium

[*]Corresponding author. Tel.: +32 9 264 57 40; fax: +32 9 264 58 46.
E-mail address: Karen.DeClerck@ugent.be (K. De Clerck).

Abstract

Delamination and brittle matrix fracture has since long been a problem of fibre reinforced composites. This paper investigates if polycaprolactone (PCL) nanofibre nonwovens can increase the interlaminar fracture toughness of resin transfer moulded glass fibre/epoxy laminates, without causing problems during impregnation and without negatively affecting other (mechanical) properties.

The mode I fracture toughness was shown to be dependent on both the nanofibre content as well as on how the nanofibres were introduced into the laminates. Almost 100% improvement in fracture toughness could be achieved by electrospinning the PCL nanofibres on both sides of the glass fibre mats prior to impregnation. This led to a mode I fracture toughness of over 1200 J/m^2.

Tensile and dynamic mechanical properties of the toughened laminates were not affected by the PCL nanofibres. It could be concluded that even state of the art infusion resins with a high intrinsic fracture toughness can benefit significantly from nanofibre toughening.

Keywords A: Nano composites, E: Resin transfer moulding (RTM), B: Delamination, B: Fracture toughness

1 Introduction

Delamination and brittle matrix fracture has since long been a problem of fibre reinforced composites [1-3]. A lot of research has been devoted to prevent delamination by modifying the epoxy matrix, either by chemically modifying the resin and hardener components, e.g. by using dendritic hyper branched polymers [4], or by adding additional components to the epoxy resin, e.g. mixing in rubber particles or creating specific thermoplastic phase morphologies in the matrix [5-12]. Although creating a rubbery phase inside of the epoxy matrix often increases the fracture toughness of the laminates, this increase is often accompanied with a decrease in other mechanical properties such as stiffness and strength. In the research of M.R. Dadfar et al. the mode I interlaminar fracture toughness (G_{Ic}) of the glass epoxy laminates increased from 220 J/m^2 to about 500 J/m^2 whereas the elastic modulus and tensile strength went down from 28.4 GPa to 17.8 GPa and 584 MPa to 489 MPa respectively [12]. More recently, the effect of nanoparticles such as nanoclay, carbon nanotubes, nanowhiskers and vapour grown carbon nanofibres on the toughness of the epoxy matrix has been studied [13-15]. Although an increase in bulk fracture toughness could often be accomplished by adding these additional components to the epoxy matrix, the absolute increase in interlaminar fracture toughness of the composite laminates remains moderate at best [16-18]. For example, Masahiro Arai et al. could improve the mode I initiation interlaminar fracture toughness ($G_{Ic,ini}$) of carbon fibre epoxy laminates from 200 J/m^2 to approximately 300 J/m^2 whereas the propagation fracture toughness (G_{Icprop}) increased form 500 J/m^2 to 650 J/m^2. W.X. Wang et al. obtained an increase in G_{IC} from 140 J/m^2 to 220 J/m^2 using nanowhiskers [17, 18]. In addition, all the toughening systems mentioned above have two

common disadvantages: (1) it is difficult to get a homogeneous dispersion of extra phases into the epoxy matrix and final laminate, and (2) the resin viscosity increases tremendously when these phases are mixed into the resin prior to moulding. These problems are of course very problematic for all infusion applications, such as resin transfer moulding (RTM).

Thermoplastic nanofibrous structures could offer a solution for the increased viscosity and the inhomogeneous dispersion, as nanofibre nonwovens can be readily deposited in between the primary reinforcing fibre layers prior to infusion. Thus, the viscosity of the epoxy resin is not affected. Although the idea of using electrospun nanofibres as a secondary reinforcement in composite structures has already been proposed by Dzenis and Reneker in 1999 [19], it is only since the last few years that the interlaminar toughening effects of thermoplastic nanofibres are being reported. Bilge et al. showed that P(St-co-GMA) nanofibrous interlayers can improve the open hole strength of carbon/epoxy laminates [20]. Palazetti et al. reported about the use of nylon 6.6 nanofibrous mats to increase the interlaminar properties and impact resistance of composites. The G_{Ic} increased from 473 J/m^2 to 496 J/m^2 [21, 22]. Jin Zhang et al. showed that G_{Ic} of a carbon fibre epoxy laminate could be increased from 175 J/m^2 to about 320 J/m^2 (depending on nanofibre diameter and interlayer thickness) using polyetherketone cardo nanofibres [23]. Gang Li et al. used polysulfone (PSF) nanofibres to increase the G_{Ic} of carbon fibre epoxy laminates from 310 J/m^2 up to 870 J/m^2. Furthermore, it was shown that the use of PSF nanofibrous nonwovens leads to a more efficient toughening than the use of PSF films of equal weight [24].

All research papers mentioned above used prepreg material on which the nanofibres were deposited. Although prepreg materials are often used in industry, e.g. aerospace industry almost exclusively uses prepreg materials, resin infusion has substantially gained importance for the production of big composite parts such as windmill blades and yacht parts. Modern infusion moulded laminates make use of low viscosity and high toughness epoxy resins. The mode I interlaminar fracture toughness of these laminates is typically higher than 600 J/m^2. This fracture toughness is much higher than that of the prepreg materials studied so far in literature [20-24].

This paper aims to investigate if high toughness polycaprolactone (PCL) nanofibre nonwovens can increase the interlaminar fracture toughness of these infusion moulded laminates even more, without causing problems during infusion and without negatively affecting other (mechanical) properties of the laminates.

2 Materials and methods

2.1 Materials

All composite laminates were reinforced with unidirectional E-glass fabric (Roviglas R17/475). The reinforcement had a weight of 475 g/m² in the fibre direction and a weight of 17 g/m² in the perpendicular direction.

The epoxy resin was composed of EPIKOTE resin MGS RIMR 135 with EPIKURE curing agent MGS RIMH 137 (Momentive). This is an infusion resin designed for windmill applications and it has a low viscosity and a high toughness.

Polycaprolactone pellets and solvents 98 v% formic acid and 99.8 v% acetic acid were supplied by Sigma–Aldrich and used as received.

2.2 Electrospinning

Prior to electrospinning, an appropriate solvent system was selected to allow for the production of nanofibre nonwovens in a stable and reproducible way. Furthermore the toxicity of the solvent system should be low, in order to make the system relevant for industrial application.

PCL can be electrospun in a stable and reproducible manner from a 1:1 formic acid/acetic acid solution which has a relatively low toxicity [25, 26]. Therefore, 14 wt% of PCL was dissolved in a 1:1 solution of formic acid and acetic acid. To obtain large uniform nanofibrous nonwovens, the nanofibres were produced using a multi-nozzle electrospinning set-up. This multi-nozzle method, an in house developed technology [22], diverges from a mono-nozzle set-up mainly by the number of nozzles, the general methodology itself is identical. It consists out of 32 nozzles, each fed by 16

syringes. The nozzles are placed in 4 alternating rows which have a movement in the transverse direction to ensure uniform deposition of nanofibres. In the meantime, a grounded collector is moving in the longitudinal or production direction. The speed of the groundcollector is adjusted to obtain the required areal density of the nanofibrous nonwovens. All nanofibrous nonwovens were spun in a conditioned room at 23 ± 2 °C and 50 ± 5 % RH. The tip-to-collector distance was 12.5 cm and the flow rate was set at 1 ml/h (per nozzle). The voltage was set between 20 kV and 25 kV until a stable process was achieved. Nanofibrous structures were both produced as stand-alone structures as well as deposited structures. The stand-alone nanofibrous nonwovens were electrospun on an aluminium foil, and were peeled off afterwards. The deposited structures were directly electrospun onto glass fibre mats. In both cases the fibre diameter of the nanofibrous structures was 400 ± 100 nm**.**

2.3 Vacuum assisted resin transfer moulding and preparation of PCL toughened laminates

The composite laminates were manufactured by vacuum assisted resin transfer moulding (VARTM). The glass fibre mats were stacked into a steel mould, either in a $[0°]_8$ or in a $[0°/90°]_{2s}$ configuration. All laminates consisted out of 8 layers of glass fibres and had a total thickness of 3 ± 0.1 mm. Three different configurations were used to introduce the nanofibres into the laminates. In addition to these three configurations, reference samples were produced containing only glass fibres.

In the first configuration a single layer of nanofibres was directly electrospun on one side of the glass fibre mats. These mats are stacked on top of each other. Hence, the interlayer of two neighbouring plies contains a single layer of nanofibre nonwoven. This configuration will be referred to as the single layer deposited configuration (SLD).

The second configuration, referred to as the double layer deposited configuration (DLD), consists out of one layer of nanofibres electrospun on each side of the glassfibre mats. Therefore, the interlayer of two neighbouring plies contained two layers of nanofibres on top of each other.

The third configuration was named the interlayered configuration (IL). This configuration consists of standalone nanofibre nonwovens placed in between the glass fibre mats. Therefore, the interlayer contains one layer of nanofibrous nonwoven, but that layer is not directly electrospun onto the glass fibre mats.

The samples prepared for the tensile tests contained nanofibrous nonwoven, according to the above configurations, in each interlayer. For the double cantilever beam samples (DCB), the nanofibrous nonwoven was incorporated in the tested interlayer.

Prior to infusion, the resin and hardener were mixed in a 100:30 mass ratio. A mechanical stirrer was used to ensure good mixing of resin and hardener. After mixing, the epoxy resin was placed under vacuum for 15 min to remove any air introduced during mixing.

After injection, the glass-epoxy laminate is first cured at room temperature for 24 hours and then post-cured for 15 hours at 80 °C. It should be noted that although the temperature in the post curing step is above the melting region of PCL (approximately at 60 °C) the curing at room temperature is well below the melting region[27].

2.4 Characterisation

Scanning electron microscopy (SEM, Joel Quanta 200 F FE-SEM) was used to investigate the fibre diameter of the electrospun nanofibres as well as the delamination fracture surface of the laminates. Prior to the SEM-measurements, the specimens were coated by a gold sputter coater (Balzers Union SCD 030). An optical microscope, an Olympus BX51 with an Olympus UC30 camera, was used to visualise delamination cracks in the cross section of the composite laminates as well as to determine the thickness of the interlayer between two neighbouring plies.

Mode I delamination fracture toughness was measured by DCB experiments on an electromechanical Instron 5800R machine following the ASTM D 5528 (2013) standard. Five samples were tested for each configuration. All DCB experiments were performed on unidirectional laminates and piano hinges were used to transfer the load to the sample. The

dimensions of the DCB samples were 20 x 160 x 3 mm and the initial delamination length was 50 mm and was created using a release film with a thickness of 30μm. The crack propagation in the DCB samples was followed using a traveling microscope. Throughout this paper, different cross sections of these DCB samples will be shown, a coordinate system is used to indicate the glass fibre direction (X), the direction perpendicular to the unidirectional glass fibres (Y) and the thickness direction (Z).

Tensile tests and open hole strength tests on the composites were performed on an electromechanical Instron 5800R machine with a load cell of 100 kN following the ASTM D3039/D3039M standard. The tests were displacement controlled with a speed of 2 mm/min and both displacement and load were recorded.

The $[0°/90°]_{2s}$ tensile specimens were instrumented with an extensometer to measure the longitudinal strain. The $[+45°/-45°]_{2s}$ tensile specimens were instrumented with two strain gauges to measure shear. All signals were sampled on the same time basis. The nanofibre containing tensile specimens had a DLD configuration and contained 10 g/m^2 or 20 g/m^2 of PCL nanofibres in each interlayer. Four samples were tested for each of these configurations.

The $[0°/90°]_{2s}$ open hole strength specimens had a width of 36 ± 0.5 mm and a central hole of 8 ± 0.1 mm in diameter. Three samples were tested for each configuration. The nanofibre containing open hole specimens had a DLD configuration and contained 5 g/m^2 or 20 g/m^2 of PCL nanofibres in each interlayer.

The dynamic mechanical analysis (DMA) was executed on a Q800 from TA Instruments. Before the start of the DMA experiments, a complete calibration was carried out; the temperature calibration was performed using an indium standard. Due to the high modulus of the samples, the experiments were carried out with a single cantilever clamp. The frequency was kept constant at 1 Hz and the displacement amplitude was set to 20 μm. The experiments started with bringing the

DMA-temperature to 30 °C followed by an equilibration time of 15 min, after which the temperature was raised at 2.5 °C/min to 150 °C. At least 3 samples were tested for each configuration.

3 Results and discussion

3.1 Expressing the nanofibre content

In composite materials, the fibre content is seen as a very important material parameter. There are different ways in which the nanofibre content can be expressed. In this paper, the areal density of the nanofibre nonwovens is used as a main parameter to indicate the nanofibre content. This has several advantages over other parameters such as the weight fraction to the total composite weight or to the resin weight. Areal density allows for easy comparison independent of the resin or primary reinforcing fibre density. In addition, a nanofibre weight fraction to the matrix weight does not take the positioning of the nanofibres in the interlayers into account. Indeed, the nanofibres are mainly present in the interlayers and not, or at least to a much lesser extent, in between the reinforcing fibres. Therefore, properties of a pure epoxy/nanofibre bulk material with the same weight fraction to resin content as in the laminate cannot be compared to what is present in the interlayer. To avoid this problem, the weight fraction of the nanofibres compared to the resin present in the interlayer may be used. Table 1 shows the different areal densities used and their corresponding calculated fibre fractions in the interlayer as well as the fraction of the nanofibres to the resin weight and to the total weight of the laminates for the SLD and DLD configuration.

3.2 Effect of PCL nanofibres on the resin infusion process

All laminates were produced using vacuum assisted resin transfer moulding. The viscosity and reactivity of the epoxy resin are of major importance for all infusion moulded parts. The PCL nanofibres had no measurable influence on this infusion process. The low viscosity infusion resin could easily impregnate all nanofibrous nonwovens in the interlayers. Visual examination and microscopic images showed no dry spots in the final laminates (the epoxy resin is transparent), see section 3.4.

3.3 The effect of nanofibre nonwoven placement on the interlaminar fracture toughness

Three different configurations (single layer deposited (SLD), double layer deposited (DLD) and interlayered (IL) were tested in comparison to the reference configuration without nanofibres.

Figure 1.A shows the mode I fracture toughness for the three different nanofibre stacking configurations as a function of the crack length. These values were calculated according to ASTM D 5528 from the load displacement curve (Figure 1.B) and the measured crack length recorded by a traveling microscope. The nanofibre content in the interlayer was 5 g/m^2 for each configuration implying that the DLD samples had 2.5 g/m^2 of nanofibres in each deposited nanofibre layer.It can be noted that both the IL configuration as well as the SLD configuration only show a marginal improvement over the reference laminates. In contrast the DLD configuration showed a substantial improvement. Both the initiation fracture toughness ($G_{Ic,ini}$) and the propagation fracture toughness ($G_{Ic,prop}$) were increased by about 430 J/m^2 and 280 J/m^2 respectively compared to the reference laminate. Taking into account that due to the selection of a high toughness infusion resin, the reference material already had a $G_{Ic,ini}$ of 640 ± 60J/m^2**,** the mode I initiation fracture toughness of the DLD configuration was found to be as high as 1070 ± 130 J/m^2**.**

An explanation for the remarkable difference between these configurations is found by visually examining the fracture surface of the DCB samples. Figure 2 shows a comparison between a SLD configuration and a DLD configuration. For the SLD configuration, the PCL nanofiber layer can be found on the fractured sample half that contained the glass fibre mat on which the PCL nanofibres were deposited. Therefore, the delamination crack propagated between the embedded nanofibrous layer and the glass fibre mat directly above it**.** The microscopic analysis also supports this hypothesis**,** see Section 3.4**.** It is assumed that a better adhesion/interaction of the nanofibres with the glass fibres in case the nanofibres are directly deposited on top of the glass fibres during the electrospinning process is the reason for the crack propagating above the toughened nanofibre layer. As such, the delamination crack did not go through the toughened interlayer. Hence, only marginal improvement compared to the reference was found.

In contrast, for the DLD configuration, parts of the embedded nanofibrous layer can be found on both halves of the fractured sample. This indicates that the delamination crack propagated, at least partially, through the toughened interlayer. Therefore, in the DLD configuration, more energy was required for the delamination crack to propagate through the nanofibre toughened interlayer, and hence, the fracture toughness of the DLD configuration is significantly higher than the SLD configuration.

In a DCB experiment, a release film is used to initiate the delamination in between the central plies of the laminate. Thus the film was on top of the nanofibrous nonwoven for the SLD configuration, whereas for the DLD configuration, the film was in between two nanofibrous layers. To verify the film placement had no effect on the observed differences between the SLD and DLD configurations, modified DCB specimens were designed in which there was a 1mm gap between the nanofibrous reinforcement and the release film. Thus the delamination crack started in front of the nanofibrous reinforcement. No difference in mode I fracture toughness was found for these modified specimens compared to the standard designed specimens. Again a substantial improvement for the DLD configuration was observed compared to the other configurations.

3.4 Microscopic analysis of the fracture behaviour

SEM images were taken from the fracture surfaces of the DCB samples, see Figure 3 and Figure 4. In addition, optical microscopy was used to analyse the cross section of these samples. The images were taken just before the tip of the crack path and perpendicular to the glass fibre orientation and crack propagation direction, Figure 5.

Figure 3 illustrates imprints of the PCL nanofibres, indicating the nanofibrous structure is at least partially maintained during the impregnation and curing process. The room temperature curing step is assumed to be crucial in this perspective. During this step, a solid matrix is formed, which prevents the PCL nanofibres to mix with the epoxy matrix during the post-curing step at 80 °C, which is above the melting point of PCL.

Comparing the images of the fracture surface of a nanofibre toughened laminate, Figure 4B, to the reference laminate, Figure 4A, PCL rich zones can clearly be noted. On a macroscopic level, it is assumed that these zones represent spots where the glass fibres were strongly attached to the PCL nanofibrous web. These glass fibres in turn microscopically bridge the crack front until they are finally broken or completely pulled out of the PCL rich zone. On a nano scale level, these zones contain the plastically deformed PCL and PCL nanofibres bridging matrix particles, as shown in Figure 4B. This effect is present both in the case of a DLD as well as a SLD configuration. This phenomenon could therefore explain the slightly higher fracture toughness of the single layer configuration as compared to the reference. For the DLD configuration, it is suggested that a crack path deflection during initiation has an even more important role. This is indeed illustrated in Figure 5**,** showing the crack front alternatingly propagates above and below the nanofibre toughened interlayer when a DLD configuration is used. In case of the SLD configuration, the crack path stays preferably above the nanofibrous layer. The toughening effect is also illustrated through the visual examination of the crack surface. Figure 2 shows that the PCL rich layer distribution over the two sample halves is more or less constant in the fibre direction and fluctuates mainly in the direction perpendicular to the glass fibres. It is this fluctuation that can be seen in the macroscopic images in Figure 5**,** where the crack goes through the nanofibrous layer at several locations, after which it continues on the other side of the toughened interlayer until a next jump through the interlayer occurs. From the crack surface**,** Figure 2**,** it can be noted that most of these jumps were initiated at the start of the experiment, during the initiation of the delamination crack. When the delamination crack is initiated, it will meet the PCL toughened interlayer. At this point, a crack path deflection effect is likely to occur since it requires more energy to go through the toughened interlayer than to propagate below or above it. For the SLD configuration, the delamination crack went above the toughened interlayer across the whole width of the sample. As explained in Section 3.3**,** this is most likely due to a better interaction between the nanofibres and the glass fibre mat on which they were deposited as opposed to the glass fibre mat above it. For the DLD configuration, it can be assumed that the interaction between the

nanofibrous interlayer and the top and bottom glass fibre mat is similar. As a result, the crack front does not go above the toughened interlayer across the whole width of the sample. Instead, the crack front went below or above the toughened interlayer at specific positions, depending on small variations in nanofibre to glass fibre interactions across the width of the sample. Thus the crack front had to pass through the toughened interlayer to go from one side to the other.

3.5 The effect of nanofibre content on the interlaminar fracture toughness

The nanofibre content is varied from 2.5 g/m^2 to 40 g/m^2 of PCL nanofibres in the interlayer. Figure 6 illustrates the mode I interlaminar fracture toughness of the resin transfer moulded laminates, both for the SLD and the DLD configuration.

For the SLD configuration the fracture toughness shows no important variation with nanofibre content and has a value of around 765 ± 100 J/m^2 for initiation and 1060 ± 100 J/m^2 for propagation. These values are slightly better than the 640 J/m2 and 950 J/m2 obtained for the reference laminates without nanofibres in the interlayer. It should also be noted that even though the thickness of the interlayer increases significantly when high amounts of PCL nanofibres are added to the laminate, the interlaminar fracture toughness remains almost constant. This observation supports the hypothesis that in case of a SLD configuration, the crack mainly propagates above the nanofibre layer. Hence, the obtained fracture toughness is less dependent on the nanofibre content.

For the DLD configuration, the initiation fracture toughness increases rapidly with increasing nanofibre content up to a value of 1070±130 J/m² when 5 g/m^2 of nanofibres are added in the interlayer. When more than 5 g/m^2 of nanofibres are added to the interlayer, the initiation facture toughness still increases although at a much slower rate. For the maximum value of 20 g/m^2 the initiation fracture toughness increased up to 1240 ± 170 J/m^2. This is an increase of almost 100% compared to the reference laminates. As opposed to the initiation fracture toughness, the propagation fracture toughness is shown to be relatively independent of the nanofibre content. The

propagation fracture toughness is approximately 1200 J/m^2 for all nanofibre contents. This is around 250 J/m^2 higher compared to the reference laminates. Overall it is clear the fracture toughness of the laminate increased significantly when a DLD configuration is used.

3.6 Effect of PCL nanofibre toughening on tensile properties and open hole strength

The tensile properties and open hole strength of the DLD laminate were also evaluated and compared to the reference. Tensile tests were performed on $[0°/90°]_{2S}$ and $[+45°/-45°]_{2S}$ laminates. From these tests an elastic modulus, shear modulus, tensile strength and shear strength were calculated.

It can be noted, Table 2, that the tensile properties of the laminates where hardly affected by the presence of the nanofibres, both the tensile strength and Young's modulus are maintained. In addition an improvement in open hole strength from 360 ± 7 MPa to 387 ± 19 MPa for the 5 g/m^2 DLD configuration and to 383 ± 14 MPa for the 20 g/m^2 DLD configuration can be observed. This improvement is attributed to the fact that nanofibre toughened laminates show less delamination during the open hole test. This is clearly illustrated in Figure 7 showing two open hole samples after testing (5 g/m^2 DLD configuration). The nanofibre toughened specimen clearly shows less delamination compared to the reference sample.

3.7 Dynamic mechanical properties.

Dynamic mechanical analysis verified the PCL nanofibres had no negative effect on the modulus of the glass epoxy laminates above room temperature. The DMA curves of the nanofibre containing samples are overlapping with the reference. Thus, even above the melting point of PCL (60°C) the modulus of the nanofibre containing samples is nearly identical to the reference.

In addition the glass transition temperature of the nanofibre containing laminate, which can be evaluated from the step in the storage modulus at 77°C is identical to that of the neat glass epoxy laminate.

Conclusion

The effect of PCL nanofibres on the interlaminar fracture toughness of resin transfer moulded glass fibre epoxy laminates was studied. The infusion process is not negatively influenced by the presence of the PCL nanofibres. The way in which the nanofibres are arranged into the laminate has a major effect on the mode I fracture toughness of the laminates. A DLD configuration in which the nanofibres were directly electrospun on both sides of the unidirectional glass fibre mats is clearly superior over the other tested configurations. More specifically, the obtained improvement was a function of the nanofibre content in the DLD samples. For a nanofibre content of 20 g/m^2 in the interlayers, an improvement in initiation interlaminar fracture toughness of almost 100**%** was obtained. The initiation fracture toughness increased from 640 J/m^2 for the reference laminates to 1230 J/m² for the nanofibre toughened laminates. The improved fracture toughness of the DLD configuration was also confirmed in the open hole strength tests, where the nanofibre containing samples showed significantly less delamination around the central hole.

It can be concluded that even state-of-the-art infusion resins can benefit from nanofibre toughening. This toughening effect was attributed to a good adhesion of deposited nanofibres onto the glass fibre mats, as well as to the inherent tough and ductile properties of the PCL nanofibres themselves. It is assumed that these properties resulted in glass fibre bridging as well as a crack path deflection effect during initiation of the delamination. Due to this crack path deflection, the delamination crack propagated partially through the nanofibre toughened interlayer (in case of a DLD configuration) resulting in a significant increase in fracture toughness. The tensile, shear and dynamic mechanical properties were not significantly influenced by the presence of PCL nanofibres in the interlayers.

Acknowledgement

Financial support from The Agency for Innovation by Science and Technology of Flanders (IWT) is gratefully acknowledged. Results in this paper were obtained within the framework of the IWT Strategic Basic Research Grant 121156.

References

[1] Ye L. Role of Matrix Resin in Delamination Onset and Growth in Composite Laminates. Compos Sci Technol. 1988;33(4):257-277.
[2] Garg AC. Delamination - a Damage Mode in Composite Structures. Eng Fract Mech. 1988;29(5):557-584.
[3] Salpekar SA, Raju IS, Obrien TK. Strain-Energy-Release Rate Analysis of Delamination in a Tapered Laminate Subjected to Tension Load. J Compos Mater. 1991;25(2):118-141.
[4] Mezzenga R, Boogh L, Manson JAE. A review of dendritic hyperbranched polymer as modifiers in epoxy composites. Compos Sci Technol. 2001;61(5):787-795.
[5] Garg AC, Mai YW. Failure Mechanisms in Toughened Epoxy-Resins - a Review. Compos Sci Technol. 1988;31(3):179-223.
[6] Bascom WD, Hunston DL. Fracture of Elastomer-Modified Epoxy Polymers. Adv Chem Ser. 1989(222):135-172.
[7] Hedrick JL, Yilgor I, Jurek M, Hedrick JC, Wilkes GL, Mcgrath JE. Chemical Modification of Matrix Resin Networks with Engineering Thermoplastics .1. Synthesis, Morphology, Physical Behavior and Toughening Mechanisms of Poly(Arylene Ether Sulfone) Modified Epoxy Networks. Polymer. 1991;32(11):2020-2032.
[8] Wilkinson SP, Ward TC, Mcgrath JE. Effect of Thermoplastic Modifier Variables on Toughening a Bismaleimide Matrix Resin for High-Performance Composite-Materials. Polymer. 1993;34(4):870-884.
[9] Kunz SC, Sayre JA, Assink RA. Morphology and Toughness Characterization of Epoxy-Resins Modified with Amine and Carboxyl Terminated Rubbers. Polymer. 1982;23(13):1897-1906.
[10] Riew CK, Siebert AR, Smith RW, Fernando M, Kinloch AJ. Toughened epoxy resins: Preformed particles as toughеners for adhesives and matrices. Toughened Plastics Ii. 1996;252:33-44.
[11] Pearson RA, Yee AF. Toughening Mechanisms in Thermoplastic-Modified Epoxies .1. Modification Using Poly(Phenylene Oxide). Polymer. 1993;34(17):3658-3670.
[12] Dadfar MR, Ghadami F. Effect of rubber modification on fracture toughness properties of glass reinforced hot cured epoxy composites. Mater Design. 2013;47:16-20.
[13] Barber AH, Cohen SR, Kenig S, Wagner HD. Interfacial fracture energy measurements for multi-walled carbon nanotubes pulled from a polymer matrix. Compos Sci Technol. 2004;64(15):2283-2289.
[14] Desai AV, Haque MA. Mechanics of the interface for carbon nanotube-polymer composites. Thin Wall Struct. 2005;43(11):1787-1803.
[15] Coleman JN, Khan U, Blau WJ, Gun'ko YK. Small but strong: A review of the mechanical properties of carbon nanotube-polymer composites. Carbon. 2006;44(9):1624-1652.
[16] Zhu J, Imam A, Crane R, Lozano K, Khabashesku VN, Barrera EV. Processing a glass fiber reinforced vinyl ester composite with nanotube enhancement of interlaminar shear strength. Compos Sci Technol. 2007;67(7-8):1509-1517.
[17] Wang WX, Takao Y, Matsubara T, Kim HS. Improvement of the interlaminar fracture toughness of composite laminates by whisker reinforced interlamination. Compos Sci Technol. 2002;62(6):767-774.
[18] Arai M, Noro Y, Sugimoto KI, Endo M. Mode I and mode II interlaminar fracture toughness of CFRP laminates toughened by carbon nanofiber interlayer. Compos Sci Technol. 2008;68(2):516-525.
[19] Kim JS, Reneker DH. Mechanical properties of composites using ultrafine electrospun fibers. Polym Composite. 1999;20(1):124-131.
[20] Bilge K, Venkataraman S, Menceloglu YZ, Papila M. Global and local nanofibrous interlayer toughened composites for higher in-plane strength. Composites Part A: Applied Science and Manufacturing. 2014;58(0):73-76.
[21] Palazzetti R, Zucchelli A, Gualandi C, Focarete ML, Donati L, Minak G, et al. Influence of electrospun Nylon 6,6 nanofibrous mats on the interlaminar properties of Gr-epoxy composite laminates. Compos Struct. 2012;94(2):571-579.
[22] Palazzetti R, Zucchelli A, Trendafilova I. The self-reinforcing effect of Nylon 6,6 nano-fibres on CFRP laminates subjected to low velocity impact. Compos Struct. 2013;106:661-671.
[23] Zhang J, Lin T, Wang XG. Electrospun nanofibre toughened carbon/epoxy composites: Effects of polyetherketone cardo (PEK-C) nanofibre diameter and interlayer thickness. Compos Sci Technol. 2010;70(11):1660-1666.
[24] Li G, Li P, Zhang C, Yu YH, Liu HY, Zhang S, et al. Inhomogeneous toughening of carbon fiber/epoxy composite using electrospun polysulfone nanofibrous membranes by in situ phase separation. Compos Sci Technol. 2008;68(3-4):987-994.

[25] Van der Schueren L, De Schoenmaker B, Kalaoglu OI, De Clerck K. An alternative solvent system for the steady state electrospinning of polycaprolactone. Eur Polym J. 2011;47(6):1256-1263.
[26] Lavielle N, Popa AM, de Geus M, Hebraud A, Schlatter G, Thony-Meyer L, et al. Controlled formation of poly(epsilon-caprolactone) ultrathin electrospun nanofibers in a hydrolytic degradation-assisted process. Eur Polym J. 2013;49(6):1331-1336.
[27] Fejos M, Molnar K, Karger-Kocsis J. Epoxy/Polycaprolactone Systems with Triple-Shape Memory Effect: Electrospun Nanoweb with and without Graphene Versus Co-Continuous Morphology. Materials. 2013;6(10):4489-4504.

Figures

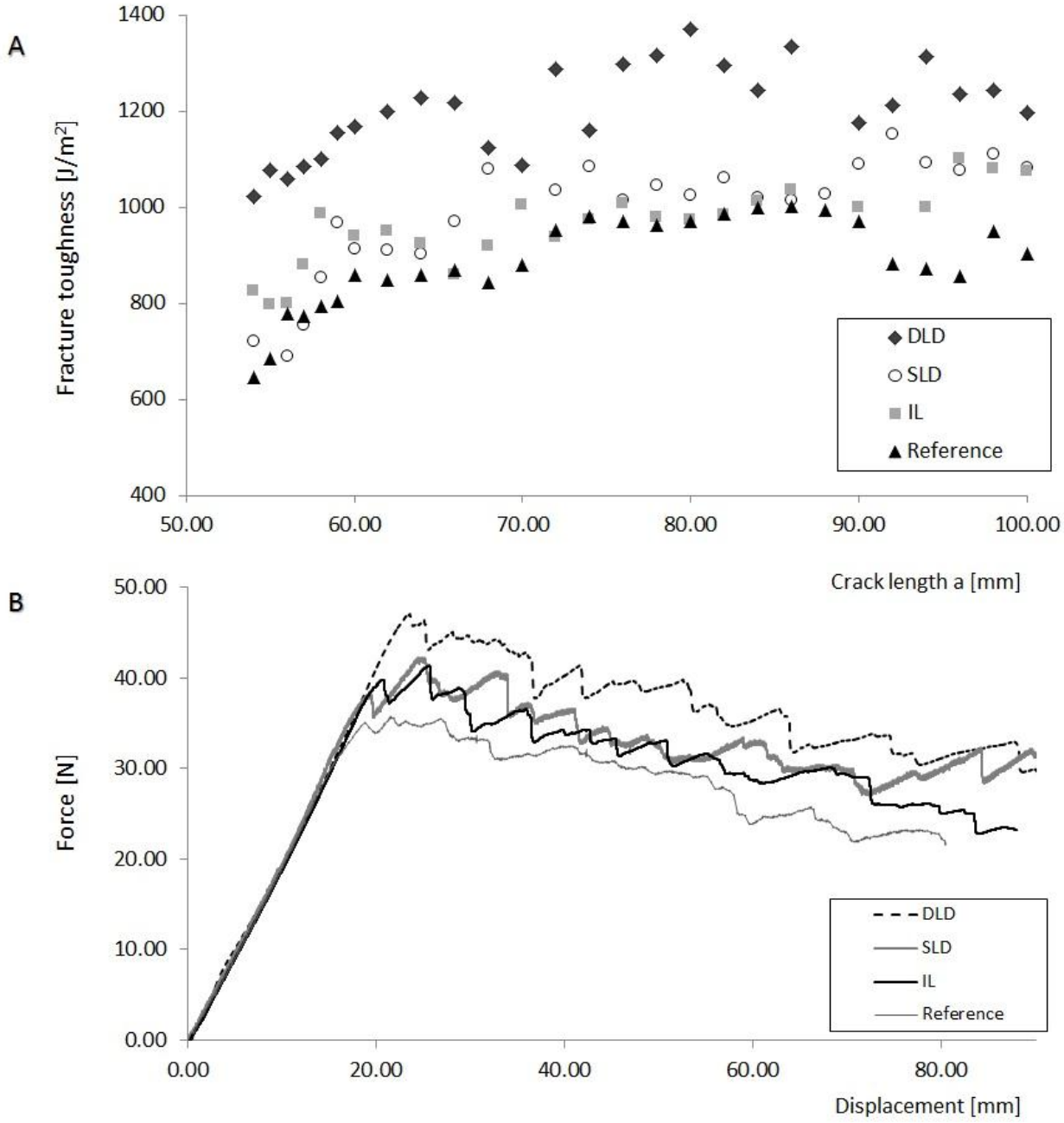

Figure 1: Mode I fracture toughness as a function of crack length (A) and load-displacement curves (B), showing significant increases when a double layer deposited (DLD) configuration is used as compared to a single layer deposited configuration (SLD) or interlayered configuration (IL).

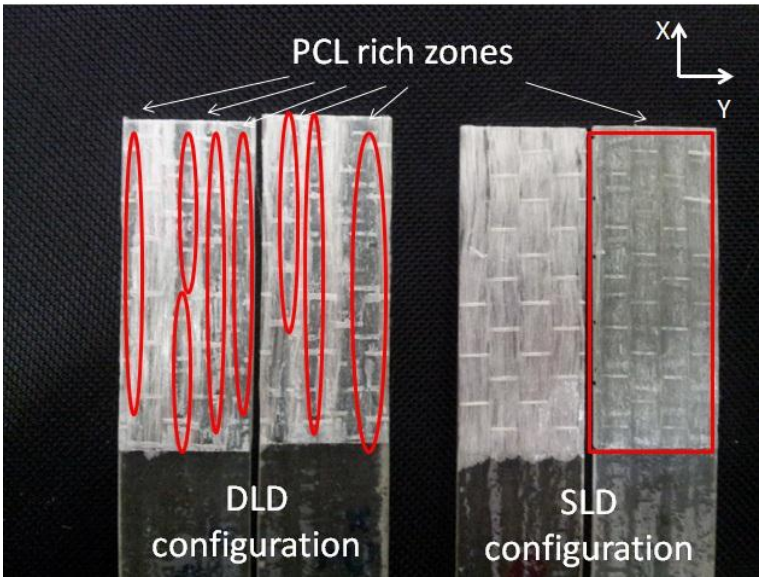

Figure 2: Fracture surface of DCB samples showing how the impregnated nanofibrous PCL nonwoven is distributed over the two sample halves after fracture in case of the DLD (left) and SLD (right) configuration.

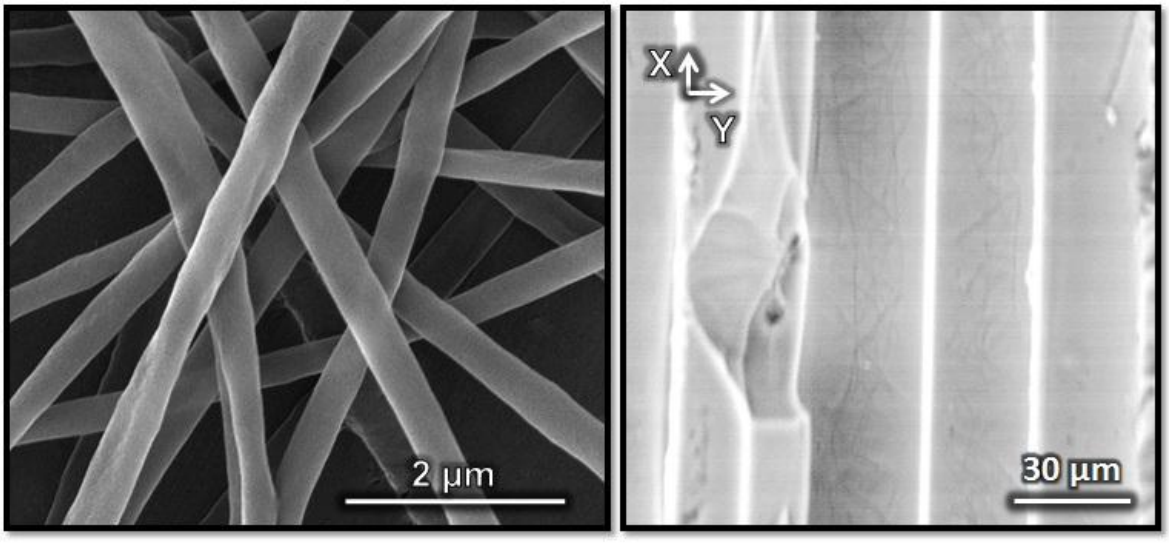

Figure 3: SEM image of PCL nanofibres (left) and a fracture surface of a DLD configuration DCB specimen showing imprints of PCL nanofibres (right).

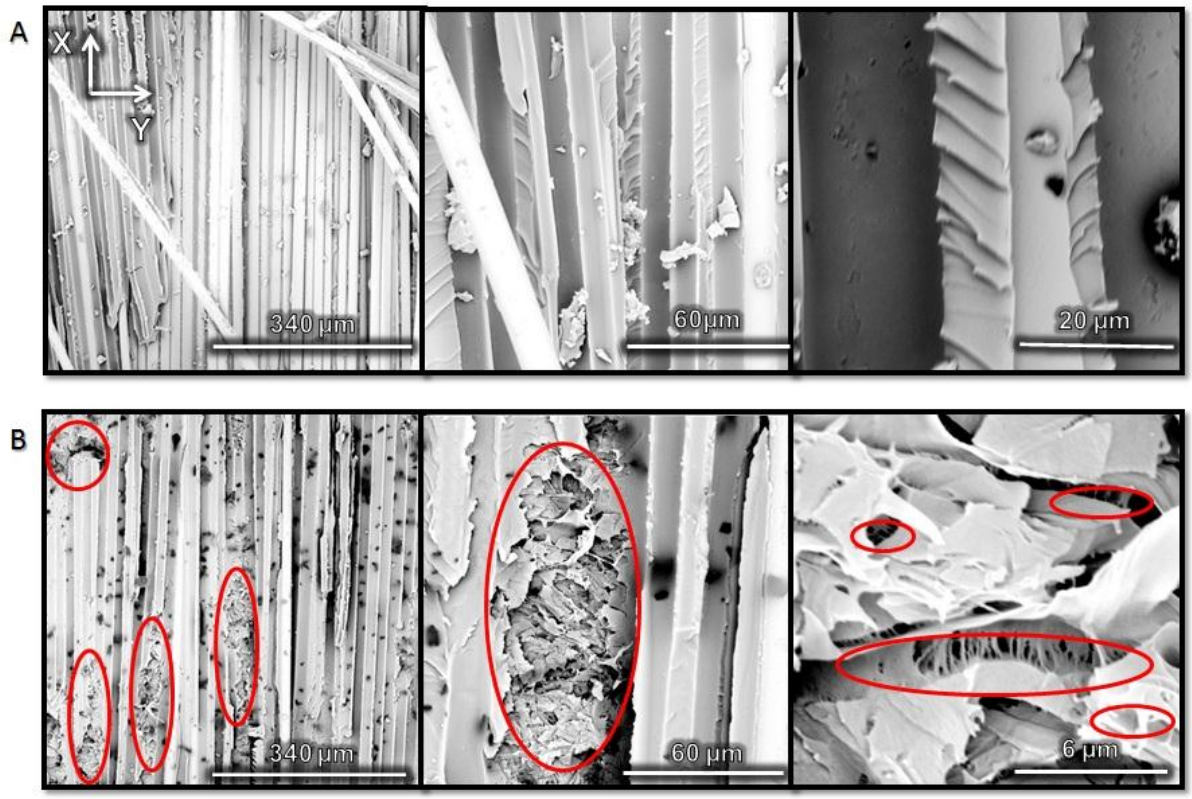

Figure 4: SEM image of reference (A) and DLD PCL nanofibre containing (B) DCB fracture surfaces. High amounts of plastic deformation and fractured pieces of epoxy matrix held together by PCL rich zones can be observed in (B).

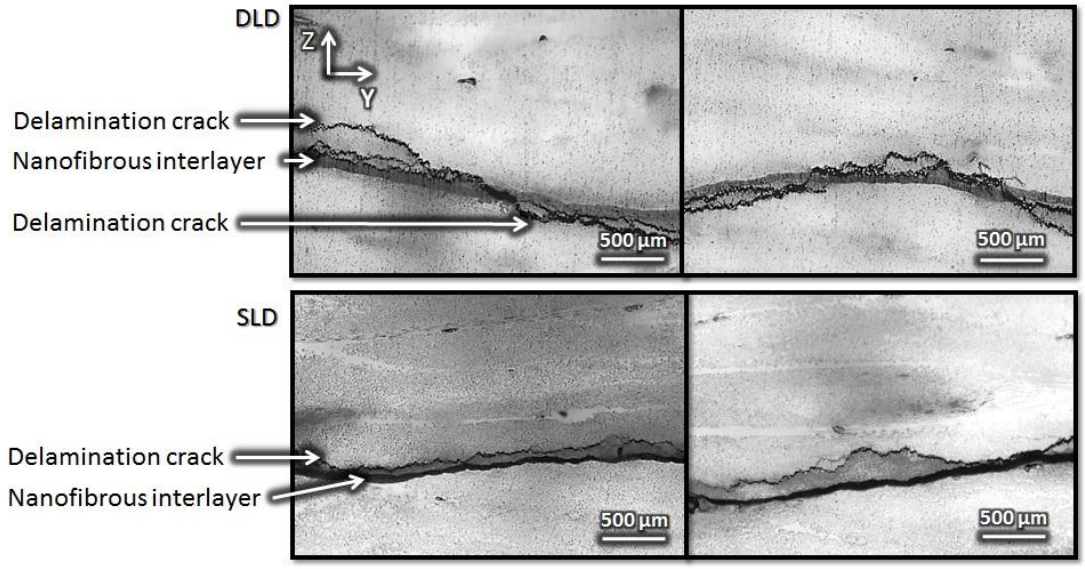

Figure 5: Cross-sectional optical microscopy images of double layer deposited configuration (DLD) and single layer deposited configuration (SLD). The crack path is perpendicular to the image plane

and goes above and below the nanofibre toughened interlayer when a DLD configuration is used.

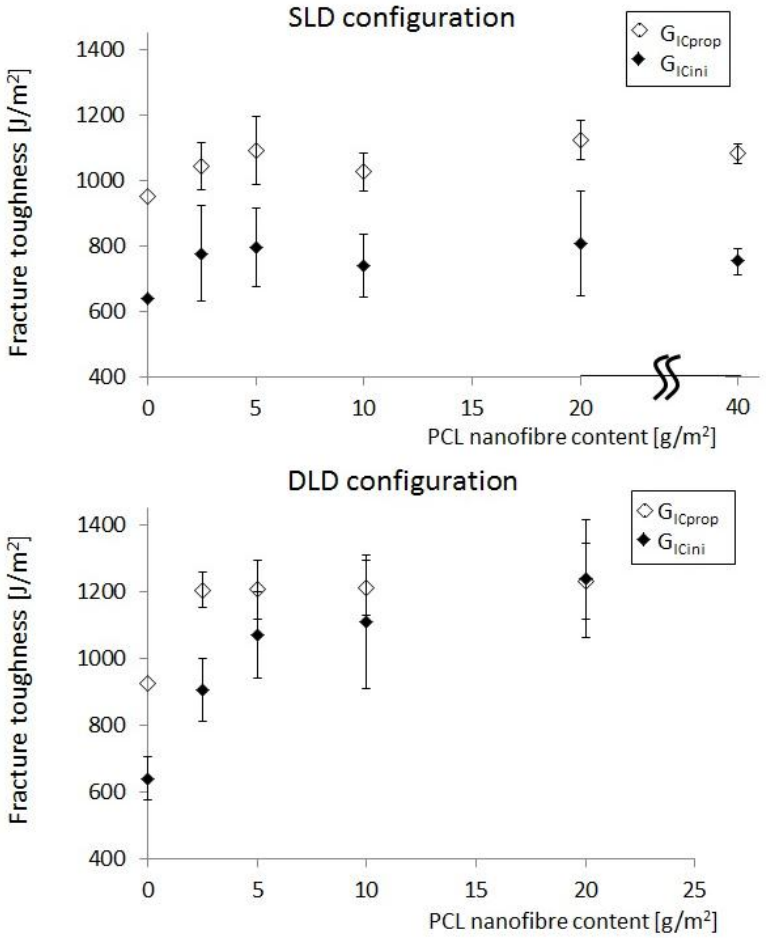

Figure 6: Effect of PCL nanofibre content on $G_{IC,ini}$ and $G_{IC,prop}$ for single and double layer deposited configurations.

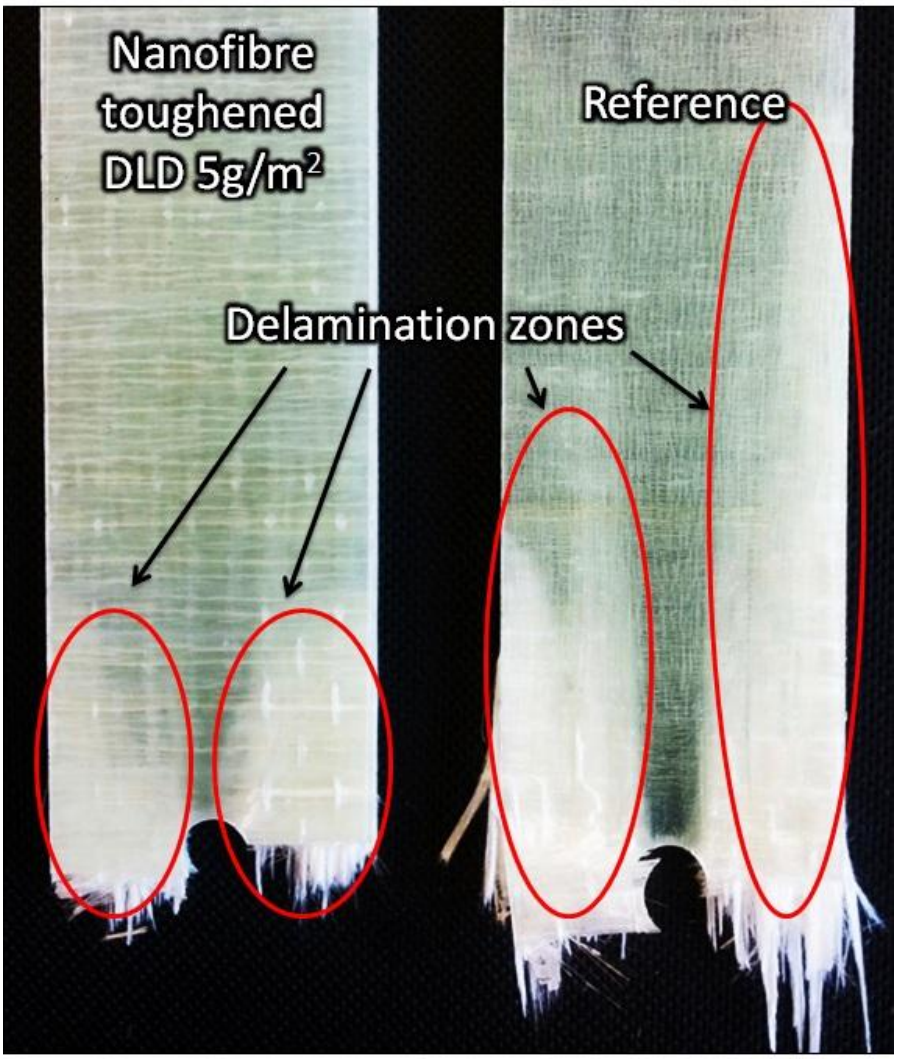

Figure 7: Open hole specimens show significantly less delamination when 5 g/m^2 of nanofibres are present in each interlayer using a DLD configuration.

Tables

Table 1: Different ways of expressing the nanofibre content of the glass-epoxy laminates.

	Areal density in interlayer (g/m^2)	**Thickness interlayer (µm)**	**wt% to resin (%)**	**wt% to resin in interlayer (%)**	**wt% to laminate (%)**
Single layer	2.5 ± 0.2	30 ± 5	0.92 ± 0.07	7 ± 2	0.26 ± 0.02
deposited	10 ± 0.5	67 ± 7	3.69 ± 0.18	13 ± 2	1.05 ± 0.05
configuration	40 ± 0.5	176 ± 12	14.77 ± 0.18	19 ± 2	4.21 ± 0.05
Double layer	2.5 ± 0.2	17 ± 5	0.92 ± 0.07	13 ± 5	0.26 ± 0.02
deposited	5 ± 0.5	43 ± 7	1.85 ± 0.18	10 ± 3	0.53 ± 0.05
configuration	10 ± 0.6	53 ± 15	3.69 ± 0.22	16 ± 6	1.05 ± 0.06
	20 ± 0.5	89 ± 15	7.39 ± 0.18	19 ± 4	2.11 ± 0.05

Table 2: Tensile properties of composite laminates show no decrease when PCL nanofibres are added (DLD configuration).

	Nanofibre content (g/m^2)	**σ_{xx} (MPa)**	**E_{xx} (GPa)**
Ref $[0°/90°]_{2S}$	0	574 ± 50	25 ± 1
Nf $[0°/90°]_{2S}$	10	596 ± 50	24 ± 1
Nf $[0°/90°]_{2S}$	20	603± 20	25± 1
		τ max (MPa)	**G_{xy} (GPa)**
Ref $[+45°/-45°]_{2S}$	0	62 ± 2	4.4 ± 0.2
Nf$[+45°/-45°]_{2S}$	10	59 ± 2	3.9 ± 0.2
Nf$[+45°/-45°]_{2S}$	20	60± 1	4.2 ± 0.2